

Cutaneous and systemic hyperinflammation drives maculopapular drug exanthema in severely ill COVID-19 patients

yasutaka mitamura¹, Daniel Schulz², Saskia Oro³, Nick Li⁴, Isabel Kolm-Djamei², Claudia Lang⁴, Reihane Ziadlou⁴, Ge Tan², Bernd Bodenmiller², Peter Steiger², Angelo Marzano⁵, Nicola de Prost³, Olivier Caudin³, Mitchell Levesque⁴, Corinne Stoffel⁴, Peter Schmid-Grendelmeier⁴, Emanuel Maverakis⁶, Cezmi Akdis², and Marie-Charlotte Brüggemann⁴

¹University of Zurich Swiss Institute of Allergy & Asthma Research

²University of Zurich

³Hospital Henri Mondor

⁴University Hospital Zurich

⁵Fondazione IRCCS Ca' Granda Ospedale Maggiore Policlinico

⁶University of California Davis

February 23, 2021

Abstract

Background Coronavirus disease 2019 (COVID-19) has been associated with cutaneous findings, some being the result of drug hypersensitivity reactions such as maculopapular drug rashes (MDR). The aim of this study was to investigate whether COVID-19 is associated with the development of the MDR. Method Blood and skin samples from COVID-19 patients suffering from maculopapular drug rashes (COVID-MDR), healthy controls, non-COVID-19-related patients with drug rash with eosinophilia and systemic symptoms (DRESS), and MDR were analyzed. We utilized imaging mass cytometry (IMC) to characterize the cellular infiltrate in skin biopsies. Furthermore, RNA sequencing transcriptome of skin biopsy samples and high-throughput multiplexed proteomic profiling of serum were performed. Results IMC revealed by clustering analyses a more prominent, phenotypically shifted cytotoxic CD8+ T cell population and highly activated monocyte/macrophage (Mo/Mac) clusters in COVID-MDR. The RNA sequencing transcriptome demonstrated a more robust cytotoxic response in COVID-MDR skin. However, severe acute respiratory syndrome coronavirus 2 (SARS-CoV-2) was not detected in skin biopsies at the time point of MDR diagnosis. Serum proteomic profiling of COVID-MDR patients revealed up-regulation of various inflammatory mediators (IL-4, IL-5, IL-6, IL-8, IL-18, TNF, and IFN- γ), eosinophil and Mo/Mac-attracting chemokines (MCP-2, MCP-3, MCP-4 and CCL11). Analyses of cytokine networks demonstrated a relatively milder cytokine storm in DRESS compared to COVID-MDR, while MDR did not exhibit such features. Conclusion A massive systemic cytokine storm may promote activation of Mo/Mac and cytotoxic CD8+ T cells in severe COVID-19 patients, which in turn may impact the development of MDR.

Title:

Cutaneous and systemic hyperinflammation drives maculopapular drug exanthema in severely ill COVID-19 patients

A short running title: (<50 characters)

hyper-inflamed drug rash in COVID-19 patients

Authors:

Yasutaka Mitamura ^{1*}, Daniel Schulz^{2*}, Saskia Oro ³, Nick Li^{4,5}, Isabel Kolm ^{4,5}, Claudia Lang^{4,5}, Reihane Ziadlou ^{4,5}, Ge Tan¹, Bernd Bodenmiller ², Peter Steiger ^{5,6}, Marzano Angelo ^{7,8}, Nicola de Prost ³, Olivier Caudin ³, Mitchell Levesque ^{4,5}, Corinne Stoffel^{4,5}, Peter Schmid-Grendelmeier ^{4,5}, Emanuel Maverakis ⁹, Cezmi A Akdis^{1,10}, Marie-Charlotte Brügggen ^{4, 5, 10}

Affiliations:

1 Swiss Institute for Allergy Research (SIAF) Davos, Davos, Switzerland

2 Institute of Molecular Life Sciences, University of Zurich, Zurich, Switzerland.

3 Department of Dermatology, Henri Mondor Hospital, Créteil, Paris, France

4 Department of Dermatology, University Hospital Zurich, Zurich, Switzerland

5 Faculty of Medicine, University Zurich, Zurich, Switzerland

6 Department of Intensive Care Medicine, University Hospital Zurich, Zurich, Switzerland

7 Dermatology Unit, Fondazione IRCCS Ca' Granda Ospedale Maggiore Policlinico, Milan, Italy

8 Department of Pathophysiology and Transplantation, Università degli Studi di Milano, Milan, Italy

9 Department of Dermatology, University of California, Davis, Sacramento, CA, USA

10 Christine Kühne-Center for Allergy Research and Education, Davos

*: The equal contributions to this work

Corresponding author:

Prof. Marie-Charlotte Brügggen; MD PhD

Department of Dermatology, Allergy Unit

University Hospital Zurich

Raemistrasse 100

CH- 8091 Zurich, Switzerland

Tel.: +41 44 255 11 11; Fax: +41 44 255 43 45

E-Mail: marie-charlotte.brueggen@usz.ch

Acknowledgements

This work was supported by the COVID-19 solidarity funds of the University of Zurich, Faculty of Medicine, and by the Christine Kühne Center for Allergy Research and education (CK Care) -Foundation. We thank Anja Heider for her help in the laboratory and Anna Głobińska for her help to prepare the graphical abstract. We thank Nils Eling of the Bodenmiller lab for his implementation of the cell-type classification.

Conflicts of Interest: None declared

IRB approval status: We have a valid ethics approval to conduct this study (EK2020-01029). All patients gave written informed consent.

Abstract (250 words)

Background

Coronavirus disease 2019 (COVID-19) has been associated with cutaneous findings, some being the result of drug hypersensitivity reactions such as maculopapular drug rashes (MDR). The aim of this study was to investigate whether COVID-19 is associated with the development of the MDR.

Method

Blood and skin samples from COVID-19 patients suffering from maculopapular drug rashes (COVID-MDR), healthy controls, non-COVID-19—related patients with drug rash with eosinophilia and systemic symptoms (DRESS), and MDR were analyzed. We utilized imaging mass cytometry (IMC) to characterize the cellular infiltrate in skin biopsies. Furthermore, RNA sequencing transcriptome of skin biopsy samples and high-throughput multiplexed proteomic profiling of serum were performed.

Results

IMC revealed by clustering analyses a more prominent, phenotypically shifted cytotoxic CD8+ T cell population and highly activated monocyte/macrophage (Mo/Mac) clusters in COVID-MDR. The RNA sequencing transcriptome demonstrated a more robust cytotoxic response in COVID-MDR skin. However, severe acute respiratory syndrome coronavirus 2 (SARS-CoV-2) was not detected in skin biopsies at the time point of MDR diagnosis. Serum proteomic profiling of COVID-MDR patients revealed up-regulation of various inflammatory mediators (IL-4, IL-5, IL-6, IL-8, IL-18, TNF, and IFN- γ), eosinophil and Mo/Mac -attracting chemokines (MCP-2, MCP-3, MCP-4 and CCL11). Analyses of cytokine networks demonstrated a relatively milder cytokine storm in DRESS compared to COVID-MDR, while MDR did not exhibit such features.

Conclusion

A massive systemic cytokine storm may promote activation of Mo/Mac and cytotoxic CD8+ T cells in severe COVID-19 patients, which in turn may impact the development of MDR.

Keywords: coronavirus, COVID-19, Drug-induced maculopapular exanthema, SARS-CoV-2,

Manuscript word count: 3482 words

References: 44

Figures: 5

Supplementary figures: 5

Tables: 2

Supplementary tables: 4

Abbreviations

COVID-19	Coronavirus disease-2019
MDR	Maculopapular drug rash
COVID-MDR	Maculopapular drug rash with COVID-19 infection
DRESS	Drug rash with eosinophilia and systemic symptoms
IMC	Imaging Mass Cytometry
SARS-CoV-2	Severe acute respiratory syndrome coronavirus 2
LC	Langerhans cells
Mo/Mac	monocyte/macrophage
DDH	Delayed-type hypersensitivity reaction
ACE2	angiotensin-converting enzyme 2
HC	Healthy controls
HE	Hematoxylin / eosin
FFPE	Formalin-fixed, paraffin-embedded
PMN	polymorphonuclear leukocytes
RNA-seq	RNA sequencing
RT-PCR	Reverse transcription polymerase chain reaction

GO BP	Gene ontology biological processes
NPX	Normalized protein expression
DC-LAMP	Dendritic cell lysosomal associated membrane glycoprotein
PCA	Principal component analysis
MCP	monocyte chemoattractant protein

Introduction

Delayed-type drug hypersensitivity reactions (DDH) result from T cell-mediated immune responses against drugs (Gell and Coombs type IV allergic reaction)¹. DDH affect about 7% of the general population^{2,3}. The most common DDH are maculopapular drug exanthemas (maculopapular drug rashes ; MDR), which are typically mild reactions that are limited to the skin and controllable with topical corticosteroids⁴. In contrast, severe cutaneous hypersensitivity reactions are rare, but life-threatening when they occur. Drug reaction with eosinophilia and systemic symptoms (DRESS) belongs to the category of severe DDH⁵.

Since the beginning of the Coronavirus disease 19 (COVID-19) pandemic⁶,

different types of DDH have been reported in severe acute respiratory syndrome coronavirus 2 (SARS-CoV-2)-infected patients⁷, raising the question as to how COVID-19 is associated with their development. We and others have reported glucocorticoid-refractory severe DRESS with massive eosinophilia in COVID-19 patients^{8,9}. Besides DDH, other cutaneous eruptions have been associated with SARS-CoV-2 infection and have been observed in approximately 1-20 % of the patients¹⁰⁻¹⁵. These various skin manifestations of SARS-CoV-2 infection^{16,17} may be due in part to the SARS-CoV-2 spike protein receptor (angiotensin-converting enzyme 2, ACE2) being expressed by keratinocytes¹⁷ Supporting this possibility is the finding that SARS-CoV-2 RNA can be directly isolated from the skin of some COVID19 patients¹⁸.

Here we report a series of MDR cases in severely ill COVID-19 patients and sought to address how MDR occurring in COVID-19 patients (COVID-MDR) differs from MDR not related to COVID, and DRESS.

Material and Methods

Study Population

We included all cases of COVID-MDR (n=12) treated in the intensive care units of two European tertiary care hospitals between March 15th and May 1st 2020 (University Hospital Zurich, and Henri Mondor Hospital, Créteil). Non COVID-19-related DRESS- (n=5; median REGISCAR score 5) and MDR-cases (n=7) with similar affected body surface areas as the COVID MDR patients (50-80%), treated in the University Hospital Zurich, were used as control groups (Table 1). Diagnoses were based on clinical assessment, identification of a culprit drug, laboratory values and skin histopathology. At the time of diagnosis/biopsy, patients had not received any treatment for their respective DDH. Clinical data were collected and presented for all patients, blood and skin samples for further analyses were only collected in the patient cohort from Zurich.

The study was conducted according to the ethical guidelines at the respective institutions and the Helsinki Declaration (EK2020-01029).

Sample preparation

Skin punch biopsies were taken from for histopathological evaluation were taken from all patients (n=12), skin punch biopsies for research purposes were available only for patients in Zurich: COVID-MDR- (n=4), MDR- (n=7) and DRESS (n=4), all obtained from the trunk. Skin from HC was obtained as discarded tissue from cutaneous surgery (n=5). Skin samples were formalin-fixed and paraffin-embedded (FFPE). Blood samples were obtained from COVID-MDR- (n=5), DRESS- (n=5), MDR-patients (n=3) and HC (n=4). Blood, collected using serum tubes, was processed immediately after collection and stored at -80 Celsius until further processing.

Blinded histopathological assessment

Slides with hematoxylin/eosin (HE)-stained skin sections (4 COVID-MDR, 4 MDR and 4 DRESS, Figure S1) were scanned and blindly evaluated by a board-certified dermatopathologist. For further details, see the Supplementary Materials and Methods.

Immunohistochemistry (IHC) stainings and quantification of CD3⁺ cells

FFPE tissue sections (4 COVID-MDR, 4 MDR, 3 DRESS and HC) were stained with an anti-ACE2 antibody (ThermoFisher, cat. no. MA5-31395, mouse IgG1, clone CL4035, 1:2000) and an anti-CD3 antibody (Dako, cat. No. M7254, clone F7.2.38, mouse IgG1, 1:50). Randomly selected images were obtained per scanned CD3-stained skin section of each donor. Representative photos are depicted in Figure S2. For further details, see the Supplementary Materials and Methods.

Imaging Mass Cytometry (IMC)

All antibodies used for IMC were titrated and validated by immunofluorescence for specific staining patterns and in IMC for co-staining with other known markers. Some antibodies were additionally tested with an antigen-binding fragment (Fab) labelling kit, used as previously described¹⁹. We designed an IMC panel consisting of 36 antibodies covering both non-leukocytic and leukocytic, mostly T cell- and antigen presenting cell-related, antigens (Table 2). We stained and processed COVID-MDR (n=4), DRESS (n=4), MDR (n=4), and HC (n=4) skin sections. For further details, see the Supplementary Materials and Methods.

IMC data analysis

Pre-processing and single-cell segmentation was performed following the instructions on the Bodenmiller Github repository (<https://github.com/BodenmillerGroup/ImcSegmentationPipeline>).

After single-cell generation all subsequent analysis were performed using R bioconductor. For cell-type annotation we manually gated major cell-types of interest using the cytomapper R package²⁰. The following markers were used to define cell-types: CD8⁺T cells I (CD3⁺, CD8⁺), CD4⁺ T cells I (CD3⁺, CD8⁻ CD4), keratinocytes I (E-cadherin⁺, Filaggrin⁻), keratinocytes II (Filaggrin⁺), Langerhans cells (LC; E-cadherin⁺, Langerin⁺), macrophages (CD163⁺), neutrophils (polymorphonuclear leukocytes (PMN); MPO⁺), plasmacytoid dendritic cells (pDC; CD303⁺), vasculature (CD31⁺). Roughly, half of all cells were manually gated using the markers from above. For the remaining cells in the dataset we used a random forest classifier to assign cell-types based on uniquely labelled cells²¹. Therefore, all labelled cells were split in training and test data (70:30). A random forest model was trained on the training-set (10 fold cross-validation, mtry parameter optimization) and the model performance validated on the test-set. After prediction of a cell-type for all unlabeled cells the classification results were inspected on images and additional rounds of cell labelling performed if needed. We excluded 1 HC sample, since it contained highly increased numbers of CD3⁺ T cells and was obtained from an excision of peritumoral tissue.

Cellular interactions were quantified using our published neighborhood algorithm²² and a R implementation thereof (<https://github.com/BodenmillerGroup/neighborhood>). All R code used for IMC data analysis in this study is available via our github (https://github.com/BodenmillerGroup/Skin_rash).

RNA extraction and sequencing of skin biopsies

RNA was extracted from FFPE skin biopsies of 5 HC skin samples and lesional skin biopsies of MDR (n=7) and COVID-MDR (n=3) patients with a Qiagen® RNeasy FFPE Kit. Library preparation for RNA-seq was performed by using the TruSeq Stranded RNA library preparation kit (Illumina) from total RNA. Sequencing was performed on the Illumina NextSeq 500 platform. For further details, see the Supplementary Materials and Methods.

SARS-CoV-2 RT-PCR from lesional skin

Reverse transcription polymerase chain reaction (RT-PCR) for detection of SARS-CoV-2 was run according to the manufacturer's instructions (Applied Biosystems™ Multiplex TaqMan 2019-nCoV Assay Kit v2

research use only (R.U.O.) kit - TF-MultiPlex (Cat. No. A47813/A47814). QuantStudio 5 real-time PCR-System (Applied Biosystems, Switzerland) was used and data were analyzed with the Design and Analysis Software DA 2.4 (Applied Biosystems).

High-throughput targeted proteomics from serum

Serum samples (4 COVID-MDR, 3 MDR, 5 DRESS, 5 HC) were analyzed using the inflammation panel of a proteomic multiplex assay by proximity extension assay (OLINK, Uppsala, Sweden). The proteomic multiplex assay by OLINK is a proximity extension assay with oligonucleotide-labeled antibody probe pairs that bind to their respective targets²³⁻²⁵. It measures proteins via an antibody-mediated detection system linked to synthetic DNA for quantification by a real-time polymerase chain reaction platform²⁴.

RNA-seq and proximity extension assay data analysis

A detailed description of the analysis is found in the Supplementary Materials and Methods. Genes with a p-value of less than 0.01 and log₂ fold change of greater than 0.5 or less than -0.5 ($|\text{L2FC}| > 0.5$) were included in this study (Table S1-S2).

All RNA-seq data performed in this paper can be found on the NCBI Gene Expression Omnibus (GEO) under accession number GSE161225. Enrichr, a gene list enrichment analysis tool, was utilized to search for enriched Gene ontology biological processes (GO BP). The data of a proteomic multiplex assay in Normalized protein expression (NPX) format were imported, processed by Olink-R Package (<https://github.com/ge11232002/OlinkR>). The statistical comparison of protein levels between groups was performed as previously described²⁶. The fold change and *p*-values were estimated by fitting a linear model for each protein. The statistically differentiated proteins were characterized for each sample ($|\text{L2FC}| > 1$, *p*-value < 0.05), depicted as venn diagrams, and mapped to the search tool for retrieval of interacting genes (STRING) to acquire protein-protein interaction networks.

Results

MDR in severely ill COVID-19 patients

During the first peak of the COVID-19 pandemic in March/April 2020 in Europe, we treated 12 severely COVID-19 affected patients with MDR (Table 1). Based on the clinical presentation and medication history, we made the diagnosis of a MDR. Proton-pump inhibitors were suspected as culprit drugs in 7/12 cases, antibiotics in 4 cases. Ten out of 12 patients were male, the mean age was 55 +/- 7 years. In all patients, 50-80% of the body surface area was affected (Figure 1A). A prominent eosinophilia (median: 940/mm³; range 400-6000) was present in all patients. Seven patients were treated with topical glucocorticoids (class III-IV), two with systemic glucocorticoids (methylprednisolone, 60mg). All patients recovered from the MDR after a median time of 13 days (range: 5-18). Patients had a median sepsis-related organ failure assessment score of 4 (range 2-11). Eleven patients suffered from acute respiratory distress. The median time between COVID-19 diagnosis (based on a positive nasopharyngeal SARS-CoV-2 PCR) and MDR was 25 days (range: 14-42 days).

A more prominent lymphocytic infiltrate in COVID-MDR

We first investigated the histopathological features of COVID-MDR. Blinded histopathological evaluation of HE-stained sections of COVID-MDR, DRESS and MDR did not reveal a distinct histopathological pattern (Figure S1A). However, we found a more prominent lymphocytic infiltrate in COVID-MDR. Automated quantification of an anti-CD3 IHC staining confirmed that COVID-MDR yielded a higher number of T cells (CD3⁺) in comparison to MDR, DRESS and HC (Figure 1B, C), pointing towards T cells might playing a particular role in COVID-MDR.

IMC mapping of COVID-MDR, MDR and DRESS

To explore the phenotype and topographical distribution of the T cell- and pan-leukocyte-infiltrates in COVID MDR, we designed and applied a 36 antibody-IMC panel to COVID MDR, MDR, DRESS and HC

skin sections (Table 2). After single-cell segmentation, we used a manual gating strategy to label cell-types of interest followed by classification of the remaining, unlabeled cells in the dataset (Methods). The analysis of these cell types (Figure 2A-D) showed many overlaps between the indications, but also some differences. In a quantitative comparison (Figure 2B), monocyte/macrophages (Mo/Mac) were increased in number in all three conditions (COVID-MDR, DRESS, MDR) compared to HC. CD8⁺ but not CD4⁺ T cells were more prominent in COVID-MDR than in DRESS, MDR, and HC. B cells and pDCs were generally rare in all samples (Figure 2C-D). Of note, we found that CD8⁺ T cells were often also positive for myeloid markers indicating that we do observe an overlap in markers due to low resolution and imperfect cell segmentation. Markers of T cell activation, such as GrzB also seemed elevated from some the images (Figure 2E). These results indicated a role of T cells, particularly CD8⁺ T cells and Mo/Mac in COVID-MDR.

T cell clustering: CD8⁺ T cell clusters predominate in COVID-MDR

To analyze the T cell compartment in more detail, we sub-clustered CD4⁺ and CD8⁺ T cells into 4 subsets each (Figure 3A-B, Figure S3A). Among CD8⁺ T cells, the most proliferative and cytotoxic cluster IV was increased in COVID-MDR. These cells showed strong expression of Ki67, GrzB, CD16 and the co-stimulation/activation marker CD27. Separation of CD8⁺ T cells by indication confirmed that CD8⁺ COVID-MDR T cells exhibit a more cytotoxic phenotype in comparison to MDR and DRESS (Figure S3A). All DDH showed elevated levels of CLA⁻ CD8⁺ T cells, indicating an influx of non-resident T cells into the skin (Figure 2E, Figure 3A-B). Regarding CD4⁺ T cells, no differences were observed between the DDH samples and overall frequencies were similar to HC.

Of note, in some CD8⁺ and CD4⁺ T cell clusters and especially in COVID-MDR, we observed the expression of certain myeloid markers (CD1c, CD11c, CD40, CD163) (Figure 3B). These signals are most likely observed due to low resolution of our images and the limits of cellular segmentation. Thus one can assume that T cells that express myeloid markers are in spatial proximity to myeloid cells which may be the cells that actually activate the T cells.

A particular cutaneous Mo/Mac phenotype in COVID-MDR

Next, we sub-clustered Mo/Mac into 4 subsets (Figure 3C, D). Cells of cluster III strongly expressed macrophage markers CD16, CD163, CD206 and the co-stimulatory marker CD40 all of which are associated to innate immunity. Cluster II cells expressed fewer markers, notably HLA-DR, CD163 and CD206 and lower activation. Cells of cluster IV were less activated and expressed the skin homing marker CLA. Clusters I showed low expression of other myeloid markers and HLA-DR.

Quantification of these Mo/Mac clusters (Figure 3D) revealed phenotypic diversity between COVID-MDR, DRESS, and MDR. Interestingly, Mo/Mac of cluster II were highest in COVID-MDR, but also well present in DRESS, while decreased in MDR and HC. Cells of cluster III were present in COVID-MDR and MDR but absent in DRESS and HC. A separation of Mo/Mac cells by indication confirmed the higher expression of CD1c, CD16, CD40, CD163 and CD206 in the COVID MDR Mo/Mac compartment (Figure S3B). In summary, activated macrophages expressing the co-stimulatory marker CD40 were often observed in COVID-MDR and may cause the strong activation of T cells.

Cell-cell contacts in COVID-MDR, DRESS and MDR are comparable to HC skin

We investigated the cellular contacts amount the cell-types classified in this dataset and compared them to HC samples (Figure 3E). Overall, the patterns of interaction between the indications were very similar. Despite the large differences in interaction counts, we did not observe interactions that were absent in any of the indications while present in another. We also applied our previously published neighborhood algorithm and could not detect recurrent significant changes (data not shown). We conclude that the overall cellular interactions in drug rashes stay intact given that larger amounts of immune cells are present.

Distinct gene expression features of lesional skin between COVID-MDR and MDR

Our IMC data showed a distinct CD8⁺ T lymphocyte and Mo/Mac infiltrate in COVID-MDR. To address,

whether this cellular signature was paralleled by a distinct gene expression pattern, we performed RNA-seq on RNA isolated from lesional skin.

Skin transcriptome GO analyses revealed eosinophil chemotaxis and cytolysis pathways to be activated in COVID-MDR (Figure 4A-C, Table S3). In line with our IMC results, the gene expression of GZMA, GNLY, PRF1, and CD8A was significantly upregulated in COVID-MDR compare to MDR. In addition, CCL5, CCL7, CCL13, CCL26, and IL-5 RNA levels were also upregulated in COVID-MDR. These results suggest that cytolytic processes and eosinophilic inflammation are more activated in COVID-MDR.

RNA of SARS-CoV-2 receptors but no virus in COVID-MDR lesional skin

The distinct cellular and molecular signature in COVID-MDR suggested that COVID-19 may impact this reaction in the skin. A SARS-CoV-2 PCR on RNA turned out negative for all COVID-MDR skin samples. We then investigated the expression of the known SARS-CoV-2 receptors ACE2, Transmembrane protease, serine 2 (TMPRSS2), BSG (Basigin; CD147), and DPP4 (Dipeptidyl peptidase-4, CD26)²⁷⁻²⁹. We did not find any difference in keratinocyte ACE2 expression between COVID-MDR, DRESS and MDR on a protein level by IHC staining (Figure S2). On the gene expression level however, *ACE2* and *DPP4* but not other receptor-related molecules were upregulated in COVID MDR compared to HC (Figure 4D, S4).

Systemic hyperinflammation in COVID-MDR but not MDR

The absence of viral RNA in the skin suggested that a massive systemic inflammatory response rather than SARS-CoV-2 in the skin favored the development of COVID-MDR in severely ill COVID-19 patients. We measured a panel of 92 inflammation-related proteins in the serum of COVID-MDR, MDR, and DRESS patients in comparison to HC using the proximity extension assay high-throughput proteomic platform (Table S4). Principal component analysis (PCA) of the transcriptome shows that serum samples from patients with COVID-MDR, MDR, and HC clusters were separated from each other, while DRESS had overlaps with MDR and COVID-MDR samples (Figure 5A).

Protein expression patterns of three different groups are shown in Figure 5B and 5C. There were striking differences between COVID-MDR, MDR, DRESS and HC. Increased expression of eight proinflammatory proteins overlapped in all three diseases, namely CXCL9, CXCL10, CXCL11, 4E-BP1, CDCP1, CCL20, IL-10 and IL-6. In COVID-MDR, a total of 49 proteins were significantly upregulated and 1 protein was significantly downregulated compared to HC. 24 proteins were significantly differentially expressed only in COVID-MDR (Figure 5B-C). The proteomic serum signature in COVID-MDR showed a cytokine storm. This was evidenced by a strong upregulation of inflammatory cytokines such as IL-6, tumor-necrosis factor and IL-8, type I cytokines and chemokines (interferon- γ , CXCL9, CXCL10, CXCL11), but also of mediators of a type 2 response (IL-4, IL-5, IL-13), eosinophil chemotaxis and a suppressive immune response (Figure 5D). Strikingly, DRESS shared the cytokine storm-related inflammatory cytokines and chemokines. These results are clearly indicative of systemic hyperinflammation and immune dysfunction in COVID-MDR patients, and, to a lesser extent, in DRESS (Figure S5).

Discussion

In this study, we report the clinical occurrence of MDR with high eosinophilia in severely ill COVID-19 patients and address whether MDR in severe COVID-19 patients has a cellular and molecular signature that differs from DRESS and MDR unrelated to COVID-19. IMC revealed that CD8⁺ but T cells made up the majority of the T cell infiltrate in COVID-MDR. Clustering analyses identified four CD8⁺ T lymphocyte subpopulations, with the most cytotoxic, proliferative subset being predominant in COVID-MDR. Also, Mo/Mac in COVID-MDR had a highly activated phenotype. Spatial analysis revealed that overall interactions patterns appeared similar among all indications. Mediators of cytolysis pathways and eosinophil chemotaxis were upregulated on an mRNA level in COVID-MDR skin. Proteomic immune signatures in the blood widely differed between COVID-MDR, MDR and DRESS, especially with respect to expression of eosinophil chemotaxis-, type 2 inflammation-, Innate immunity-, and immunosuppression-related proteins.

One striking finding of this COVID-MDR case series is that all patients had particularly severe COVID-

19 disease and all patients developed MDR about 1 month after their initial COVID-19 diagnosis, a time point when SARS-CoV2 is no longer detectable in nasopharyngeal swabs. SARS-CoV-2 had been previously detected in lesional skin of COVID-19 patients¹⁸ and we hypothesized that the virus might directly impact MDR development. Since SARS-CoV-2 RNA was undetectable in lesional COVID-MDR skin, we now favor an indirect impact of SARS-CoV-2 on COVID-MDR pathogenesis, possibly from peripheral immune activation. Severe COVID-19 has been associated with cytokine storm features, hemodynamic instability and multi-organ failure³⁰⁻³⁶. In line with these studies^{30,37-39}, levels of cytokine storm-associated cytokines and chemokines were highly increased in COVID-MDR. Moreover, several ‘cytotoxicity’ and ‘eosinophilic inflammation’ mediators were upregulated both in serum (protein level) and lesional skin (mRNA level) of COVID-MDR patients. These findings suggest that severe COVID-19 might impact the drug reaction through activation of cytotoxic CD8⁺ T cells, Mo/Mac and eosinophils.

By IMC, prominent CD8⁺ T cell infiltrates and highly activated Mo/Mac clusters were characteristic of COVID-MDR. Interestingly, a recent paper has identified dysfunctional HLA-DR^{low}CD163^{high} and HLA-DR^{low}S100A^{high}CD14⁺ Mo in the blood of severely affected COVID-19 patients⁴⁰. This resembles the Mo/Mac phenotype that we identified in COVID-MDR. Additional features that were unique to Mo/Mac in COVID-MDR was the very high expression of CD16, CD206, and CD11c. The role of these Mo/Mac in the pathogenesis of MDR in COVID-19 patients remains to be elucidated. Specifically, whether they promote DDH by functioning as antigen-presenting cells, or whether they are effector mediators of inflammation or even trained immunity remains to be determined.

One limitation of our study is that small sample size impacts our ability to determine the significance of the characteristic cell-cell interactions observed between diagnostic groups. Nevertheless, this study represents the first IMC neighborhood analysis in human skin. We anticipate that IMC application in other allergic and inflammatory skin conditions will shed new insights into cutaneous immune cell interactions.

Apart from contributing to the understanding of COVID-MDR, our study also provides new insights into DRESS and MDR unrelated to COVID-19. Viral reactivation, especially human herpes virus 6 or Epstein-Barr virus reactivation, are seen in about 75% of DRESS cases⁴¹. In these patients, activated peripheral CD8⁺ T lymphocytes secrete large amounts of TNF and IFN- γ ⁴¹. Our data show that DRESS is characterized by a similar systemic inflammatory response as COVID-MDR, although to a lesser extent. There is relatively little existing data about the effector immune response in DRESS, but the few studies that do exist, hint towards an aberrant T cell response, as evidenced by increased serum granzyme B⁴² and atypical T cells⁴³. Our skin IMC data did however not show prominent CD8⁺ T cell infiltrates in DRESS supports a previous finding, that CD16⁺ monocytes are depleted in DRESS lesional skin⁴⁴. Our results also show that in comparison to HC, DRESS Mo/Macs have upregulation of CD206 and CD163, and in comparison to MDR and COVID-MDR, there is an upregulation of HLA-DR and CD370.

Taken together, MDR in severely ill COVID-19 patients is likely the result of a hyperinflammatory immune response that culminates in activation of Mo/Mac and highly cytotoxic CD8⁺ T cells. These cutaneous findings are possibly initiated by or exacerbated by a robust systemic COVID-19-induced immune response. Although our characterization of the COVID-MDR was comprehensive, future studies with larger patient cohorts are needed to verify these findings.

COVID-MDR patients (n=12) at baseline

Age (years mean \pm SD)	55 \pm 7
Sex male, n	10
Ethnical origin	Caucasian n=10 Asian n=1 African n=1
Intensive care characteristics	SOFA score = 4 Mechanical ventilation n=10 ARDS n=11 ECMO n=5 Hemodialysis n=6
Type of skin lesions	Maculopapular n=11
Affected body surface area (%)	69 (51-80)

Time between COVID-19 diagnosis and MDR onset (days, median (range))	25 (14-42)
Time between drug exposure and MDR onset (days, median (range))	7 (5-30)
Length of skin lesions to resolution (days, median (range))	13 (6-18)
Treatment of MDR	Topical steroids n=7 Systemic steroids n=4
MDR patients (n=7) at baseline	MDR patients (n=7) at baseline
Age (years mean \pm SD)	52 \pm 12
Sex male, n	5
Type of skin lesions	maculopapular
Affected body surface area (%)	65 (60-80)
DRESS patients (n=5) at baseline	DRESS patients (n=5) at baseline
Age (years mean \pm SD)	47 \pm 8
Sex male, n	4
Type of skin lesions	maculopapular
Affected body surface area (%)	74 (66-80)
Regiscar DRESS score (range)	6 (6-7)

Table 1. Clinical characteristics of patients.

Target	Antibody Clone
CD20	L26
Filaggrin	AKH1
E-Cadherin_P-Cadherin	36/E-Cadherin
Ki-67	B56
Langerin	H-4
CD1c	3G1B3
CD11c	D3V1E
DC-LAMP	1010E1.01
CD68	KP1
CD163	EDHu-1
CD16	EPR16784
CD370	EPR22324
HLA-DR	TAL 1B5
CD40	EPR20735
CD14	SP192
CD206	685645
CD11b	SP330
Myeloperoxidase MPO	Polyclonal MPO
Histone H3	D1H2
DNA1	
DNA2	
CD303	Polyclonal_DLEC / CLEC4C / BDCA-2 (R&D Systems)
SMA	1A4
CD31	EPR3094
CD7	EPR4242
CD69	EPR21814
Cutaneous Lymphocyte Antigen	HECA-452
CD57	HNK-1

Target	Antibody Clone
DP2	C-5
Granzyme B	D6E9W
CD134	Ber-ACT35 (ACT35)
CD27	Polyclonal_CD27 / TNFRSF7 (R&D Systems)
CD45RA	HI100
CD45RO	UCHL1
FOXP3	236A/E7
CD8a	C8/144B
CD4	EPR6855
CD3	polyclonal_A0452 (Dako)
STING	SP339

Table 2. Antibodies used for IMC.

References

1. Peter JG, Lehloenya R, Dlamini S, et al. Severe Delayed Cutaneous and Systemic Reactions to Drugs: A Global Perspective on the Science and Art of Current Practice. *J Allergy Clin Immunol Pract.* 2017;5(3):547-563.
2. Demoly P, Adkinson NF, Brockow K, et al. International Consensus on drug allergy. *Allergy.* 2014;69(4):420-437.
3. Gomes E, Cardoso MF, Praça F, Gomes L, Mariño E, Demoly P. Self-reported drug allergy in a general adult Portuguese population. *Clin Exp Allergy.* 2004;34(10):1597-1601.
4. Wong SX, Tham MY, Goh CL, Cheong HH, Chan SY. Spontaneous cutaneous adverse drug reaction reports-An analysis of a 10-year dataset in Singapore. *Pharmacol Res Perspect.* 2019;7(2):e00469.
5. Martínez-Cabriales SA, Rodríguez-Bolaños F, Shear NH. Drug Reaction with Eosinophilia and Systemic Symptoms (DRESS): How Far Have We Come? *Am J Clin Dermatol.* 2019;20(2):217-236.
6. Zhu N, Zhang D, Wang W, et al. A Novel Coronavirus from Patients with Pneumonia in China, 2019. *N Engl J Med.* 2020;382(8):727-733.
7. Rossi CM, Beretta FN, Traverso G, Mancarella S, Zenoni D. A case report of toxic epidermal necrolysis (TEN) in a patient with COVID-19 treated with hydroxychloroquine: are these two partners in crime? *Clin Mol Allergy.* 2020;18:19.
8. Schmid-Grendelmeier P, Steiger P, Naegeli MC, et al. Benralizumab for severe DRESS in two COVID-19 patients. *J Allergy Clin Immunol Pract.* 2021;9(1):481-483.e482.
9. Balconi SN, Lopes NT, Luzzatto L, Bonamigo RR. Detection of SARS-CoV-2 in a case of DRESS by sulfasalazine: could there be a relationship with clinical importance? *Int J Dermatol.* 2021;60(1):125-126.
10. Manjaly Thomas ZR, Leuppi-Taegtmeyer A, Jamiolkowski D, et al. Emerging treatments in COVID-19: Adverse drug reactions including drug hypersensitivities. *J Allergy Clin Immunol.* 2020;146(4):786-789.
11. Novak N, Peng W, Naegeli MC, et al. SARS-CoV-2, COVID-19, skin and immunology - What do we know so far? *Allergy.* 2020; Online ahead of print.
12. Hedou M, Carsuzaa F, Chary E, Hainaut E, Cazenave-Roblot F, Masson Regnault M. Comment on 'Cutaneous manifestations in COVID-19: a first perspective' by Recalcati S. *J Eur Acad Dermatol Venereol.* 2020;34(7):e299-e300.

13. Galván Casas C, Català A, Carretero Hernández G, et al. Classification of the cutaneous manifestations of COVID-19: a rapid prospective nationwide consensus study in Spain with 375 cases. *Br J Dermatol.* 2020;183(1):71-77.
14. Riggioni C, Comberiati P, Giovannini M, et al. A compendium answering 150 questions on COVID-19 and SARS-CoV-2. *Allergy.* 2020;75(10):2503-2541.
15. Marzano AV, Genovese G, Fabbrocini G, et al. Varicella-like exanthem as a specific COVID-19-associated skin manifestation: Multicenter case series of 22 patients. *J Am Acad Dermatol.* 2020;83(1):280-285.
16. Azkur AK, Akdis M, Azkur D, et al. Immune response to SARS-CoV-2 and mechanisms of immunopathological changes in COVID-19. *Allergy.* 2020;75(7):1564-1581.
17. Xue X, Mi Z, Wang Z, Pang Z, Liu H, Zhang F. High Expression of ACE2 on Keratinocytes Reveals Skin as a Potential Target for SARS-CoV-2. *J Invest Dermatol.*2020;S0022-202X(20):31602-X.
18. Jamiolkowski D, Mühleisen B, Müller S, Navarini AA, Tzankov A, Roeder E. SARS-CoV-2 PCR testing of skin for COVID-19 diagnostics: a case report. *Lancet.*2020;396(10251):598-599.
19. Brügggen MC, Strobl J, Koszik F, et al. Subcutaneous White Adipose Tissue of Healthy Young Individuals Harbors a Leukocyte Compartment Distinct from Skin and Blood. *J Invest Dermatol.* 2019;139(9):2052-2055.e2057.
20. Eling N, Damond N, Hoch T, Bodenmiller B. `cytomapper`: an R/Bioconductor package for visualisation of highly multiplexed imaging data. *bioRxiv.* 2020:2020.2009.2008.287516.
21. M. K. Building Predictive Models in R Using the caret Package. *Journal of Statistical Software.*2008;28(5).
22. Schapiro D, Jackson HW, Raghuraman S, et al. histoCAT: analysis of cell phenotypes and interactions in multiplex image cytometry data. *Nat Methods.*2017;14(9):873-876.
23. Assarsson E, Lundberg M, Holmquist G, et al. Homogenous 96-plex PEA immunoassay exhibiting high sensitivity, specificity, and excellent scalability. *PLoS One.*2014;9(4):e95192.
24. Lind L, Ärnlov J, Lindahl B, Siegbahn A, Sundström J, Ingelsson E. Use of a proximity extension assay proteomics chip to discover new biomarkers for human atherosclerosis. *Atherosclerosis.* 2015;242(1):205-210.
25. Söderlund S, Christiansson L, Persson I, et al. Plasma proteomics in CML patients before and after initiation of tyrosine kinase inhibitor therapy reveals induced Th1 immunity and loss of angiogenic stimuli. *Leuk Res.*2016;50:95-103.
26. Lang C, Masenga J, Semango G, et al. Evidence for different immune signatures and sensitization patterns in sub-Saharan versus central European Atopic Dermatitis patients. *J Eur Acad Dermatol Venereol.* 2020.
27. Sungnak W, Huang N, Bécavin C, et al. SARS-CoV-2 entry factors are highly expressed in nasal epithelial cells together with innate immune genes. *Nat Med.*2020;26(5):681-687.
28. Radzikowska U, Ding M, Tan G, et al. Distribution of ACE2, CD147, CD26, and other SARS-CoV-2 associated molecules in tissues and immune cells in health and in asthma, COPD, obesity, hypertension, and COVID-19 risk factors. *Allergy.*2020;75(11):2829-2845.
29. Sokolowska M, Lukasik ZM, Agache I, et al. Immunology of COVID-19: Mechanisms, clinical outcome, diagnostics, and perspectives—A report of the European Academy of Allergy and Clinical Immunology (EAACI). *Allergy.*2020;75(10):2445-2476.
30. Leisman DE, Ronner L, Pinotti R, et al. Cytokine elevation in severe and critical COVID-19: a rapid systematic review, meta-analysis, and comparison with other inflammatory syndromes. *Lancet Respir Med.* 2020;S2213-2600(20):30404-30405.

31. Sinha P, Matthay MA, Calfee CS. Is a “Cytokine Storm” Relevant to COVID-19? *JAMA Internal Medicine*. 2020;180(9):1152-1154.
32. Zhou F, Yu T, Du R, et al. Clinical course and risk factors for mortality of adult inpatients with COVID-19 in Wuhan, China: a retrospective cohort study. *Lancet*.2020;395(10229):1054-1062.
33. Cummings MJ, Baldwin MR, Abrams D, et al. Epidemiology, clinical course, and outcomes of critically ill adults with COVID-19 in New York City: a prospective cohort study. *Lancet*. 2020;395(10239):1763-1770.
34. de la Rica R, Borges M, Gonzalez-Freire M. COVID-19: In the Eye of the Cytokine Storm. *Frontiers in Immunology*. 2020;11(2313).
35. Chen G, Wu D, Guo W, et al. Clinical and immunological features of severe and moderate coronavirus disease 2019. *J Clin Invest*. 2020;130(5):2620-2629.
36. Guan W-j, Ni Z-y, Hu Y, et al. Clinical Characteristics of Coronavirus Disease 2019 in China. *New England Journal of Medicine*. 2020;382(18):1708-1720.
37. Zhang JJ, Dong X, Cao YY, et al. Clinical characteristics of 140 patients infected with SARS-CoV-2 in Wuhan, China. *Allergy*. 2020;75(7):1730-1741.
38. Luo M, Liu J, Jiang W, Yue S, Liu H, Wei S. IL-6 and CD8+ T cell counts combined are an early predictor of in-hospital mortality of patients with COVID-19. *JCI Insight*.2020;5(13).
39. Zhang JY, Wang XM, Xing X, et al. Single-cell landscape of immunological responses in patients with COVID-19. *Nat Immunol*. 2020;21(9):1107-1118.
40. Schulte-Schrepping J, Reusch N, Paclik D, et al. Severe COVID-19 Is Marked by a Dysregulated Myeloid Cell Compartment. *Cell*. 2020;182(6):1419-1440.e1423.
41. Picard D, Janela B, Descamps V, et al. Drug reaction with eosinophilia and systemic symptoms (DRESS): a multiorgan antiviral T cell response. *Sci Transl Med*.2010;2(46):46ra62.
42. Yang F, Chen SA, Wu X, Zhu Q, Luo X. Overexpression of cytotoxic proteins correlates with liver function impairment in patients with drug reaction with eosinophilia and systemic symptoms (DRESS). *Eur J Dermatol*. 2018;28(1):13-25.
43. Kardaun SH, Sidoroff A, Valeyrie-Allanore L, et al. Variability in the clinical pattern of cutaneous side-effects of drugs with systemic symptoms: does a DRESS syndrome really exist? *Br J Dermatol*. 2007;156(3):609-611.
44. Ushigome Y, Mizukawa Y, Kimishima M, et al. Monocytes are involved in the balance between regulatory T cells and Th17 cells in severe drug eruptions. *Clin Exp Allergy*.2018;48(11):1453-1463.

Figure Legends

Figure 1. MDR in severely affected COVID-19 patients exhibit a prominent lymphocytic infiltrate.

A, Representative photographs of COVID-19 patients with MDR. **B**, Representative images of IHC staining of CD3⁺ T-cells (red) and ACE2 (brown) in the skin of COVID-MDR, MDR and DRESS. The scale is 100 μ m. **C**, Boxplots represent the fold-change of CD3⁺ T cell infiltrated area in the skin between the indicated donors (COVID-MDR, DRESS, MDR).

Figure 2. IMC mapping identifies predominance of CD8⁺ T cell clusters in COVID-MDR.

A, UMAP representation of all single cells depicting the different identified cell-types (upper graph) and all cells colored by indication (lower graph). **B**, Boxplots for the fractions of each cell-type per image split and colored by indication. (COVID-MDR, MDR, DRESS, HC). **C**, Heatmap of z-scored average expression for each marker and cell-type. **D**, Example images of classified cell-types in COVID-MDR, DRESS and MDR.

The scale bar (white line) is 200 μm in all images. **E**, Example images of the expression of CD3 (green), CD4 (magenta), CD8 (red), GrzB (yellow) and DNA (blue). The large images depict the overlaid colors, and the white box marks the zoomed in areas on the right side depicting the individual markers. The scale bar (white line) is 100 μm in all images.

Figure 3. Highly activated Mo/Mac clusters in COVID-MDR and interaction analyses.

A, Boxplots depicting the fraction of the indicated CD8⁺ T cell clusters (upper graph) and CD4⁺ T cell clusters (lower graph) among total cells in the different conditions (COVID-MDR, DRESS, MDR, HC). **B**, Heatmap of z-scored average expression for each marker of the clustered CD8⁺ T cells (left 4 columns) and CD4⁺ T cells clustered (right 4 columns). **C**, Heatmap of z-scored average marker expression of Mo/Mac clustered cells. **D**, Boxplots represent the fraction of the 4 Mo/Mac clusters among total cells in the different conditions (COVID-MDR, DRESS, MDR, HC). **E**, Circular string graph showing interactions between the main identified cell types in COVID-MDR, DRESS, MDR and HC (pooled per indication). We excluded Keratinocytes from the plot and also excluded one MDR sample which contained very high numbers of Neutrophils. The cell-types are individually colored and labelled on the outside of the plot. The number of interactions is also given on the outside of the plot. Interactions are depicted ingoing and outgoing for each cell-type.

Figure 4. Distinct skin transcriptomic profiles in COVID-MDR and MDR.

A, B, Expression heatmaps of **A** cytolysis-related genes (GO:0019835) and **B** eosinophils chemotaxis-related genes (GO:0048245) in the skin comparing COVID-MDR, MDR, and healthy control. **C**, Violin plots depicting the gene expression of indicated pathway related genes in the skin comparing COVID-MDR, MDR, and HC. **D**, Violin plots depicting the gene expression of COVID-19 receptor and related molecules in the skin comparing COVID-MDR, MDR, and HC. Normalized counts are shown. *: $p \leq 0.05$, **: $p \leq 0.01$, NS=not significant.

Figure 5. Strong blood cytokine storm signature in COVID-MDR.

A, 4-component PCA clustering of blood proteome differentiates between blood samples from patients with COVID-MDR, DRESS, MDR, and HC. **B**, The Venn diagram depicts the shared or unique differentially regulated proteins in the serum ($p \leq 0.05$, $|\text{L2FC}| \geq 1$) between each indicated comparison. **C**, Heatmap depicts all proteins shown in the Venn diagram. p-value and logFC between COVID-MDR and DRESS are shown in the table on the right. *: $p \leq 0.05$, **: $p \leq 0.01$. **D**, Box plots of selected inflammatory markers are shown. Normalized protein expression (NPX) are shown in Log₂ scale. *: $p \leq 0.05$, **: $p \leq 0.01$.

Supplementary Figure legends.

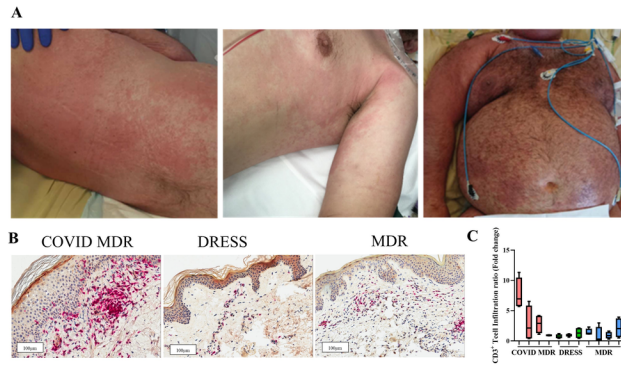
Figure S1. A, Representative pictures of H&E stainings of COVID-MDR, MDR and DRESS. The scale is 100 μm .

Figure S2. A, Images of CD3⁺ T-cells (Red) and ACE2 (brown) in the skin of COVID-MDR, MDR, DRESS and HC. Representative pictures of individual donors are depicted. The scale is 100 μm .

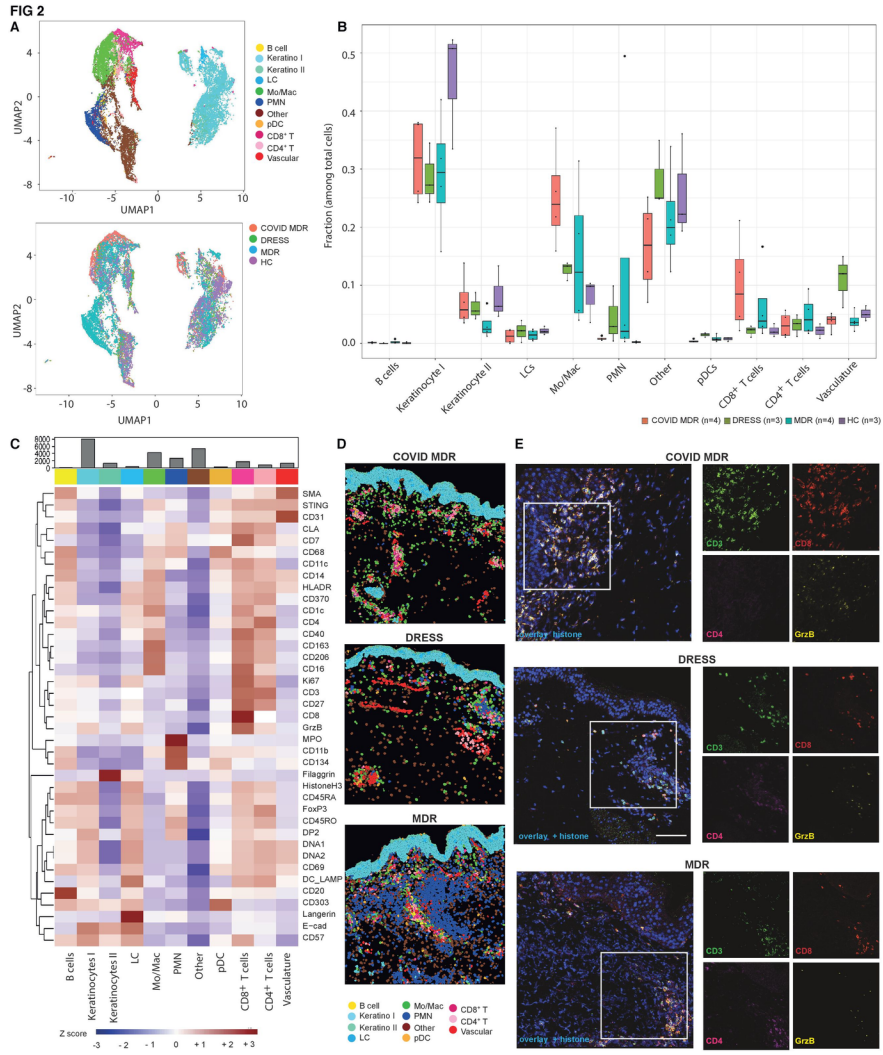
Figure S3. A, Expression heatmap of the stained antigens of CD8⁺ T cells and CD4⁺ T cells clustering per condition in COVID-MDR, DRESS, MDR and HC. **B**, Z-scored expression heatmap of the stained antigens of Mo/Mac clustering per condition in COVID-MDR, DRESS, MDR and HC.

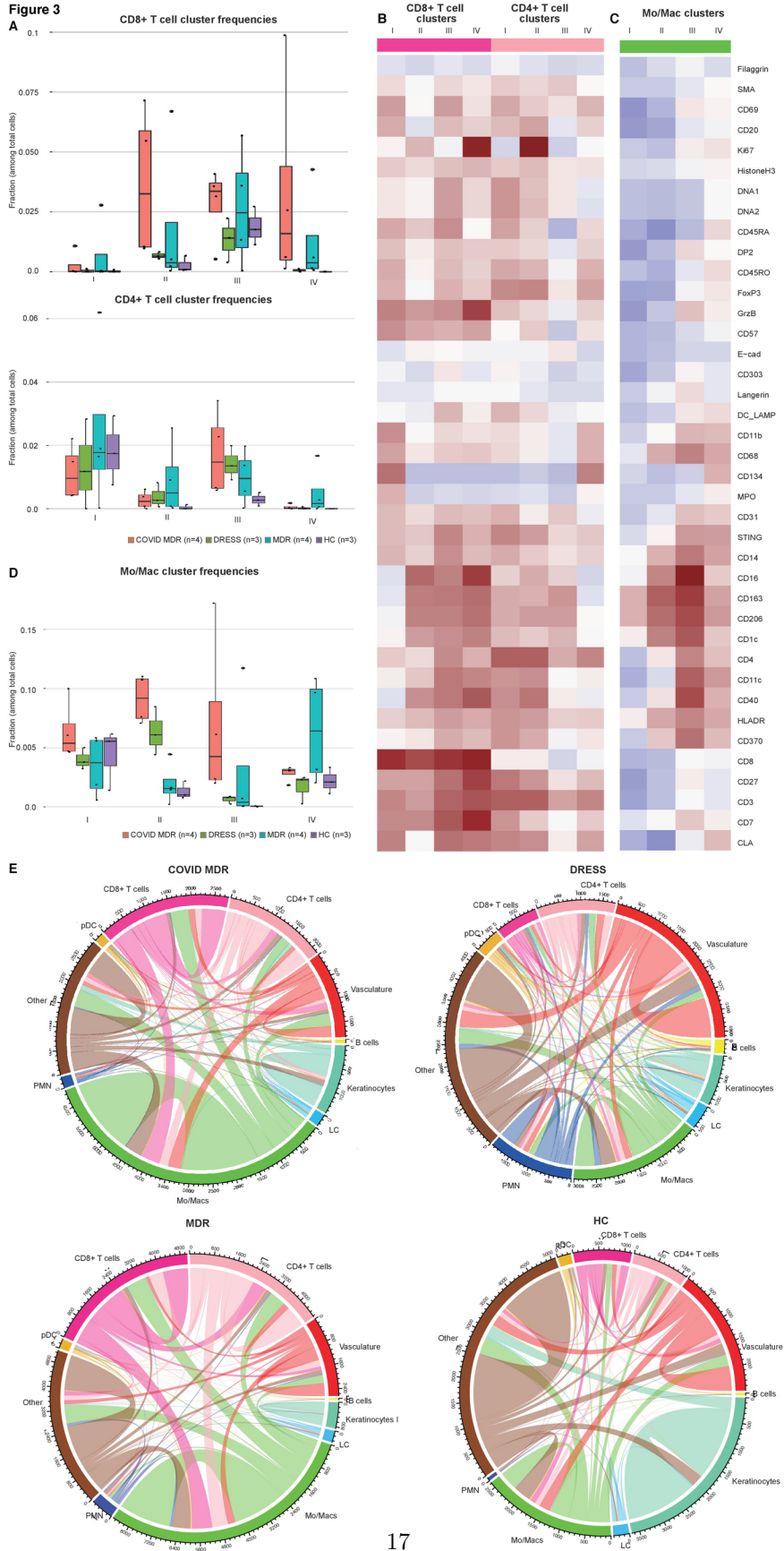
Figure S4. Violin plots depicting the gene expression of COVID-19 receptor-related molecules in the skin comparing COVID-MDR, MDR, and HC. *: $p \leq 0.05$, **: $p \leq 0.01$, NS=not significant.

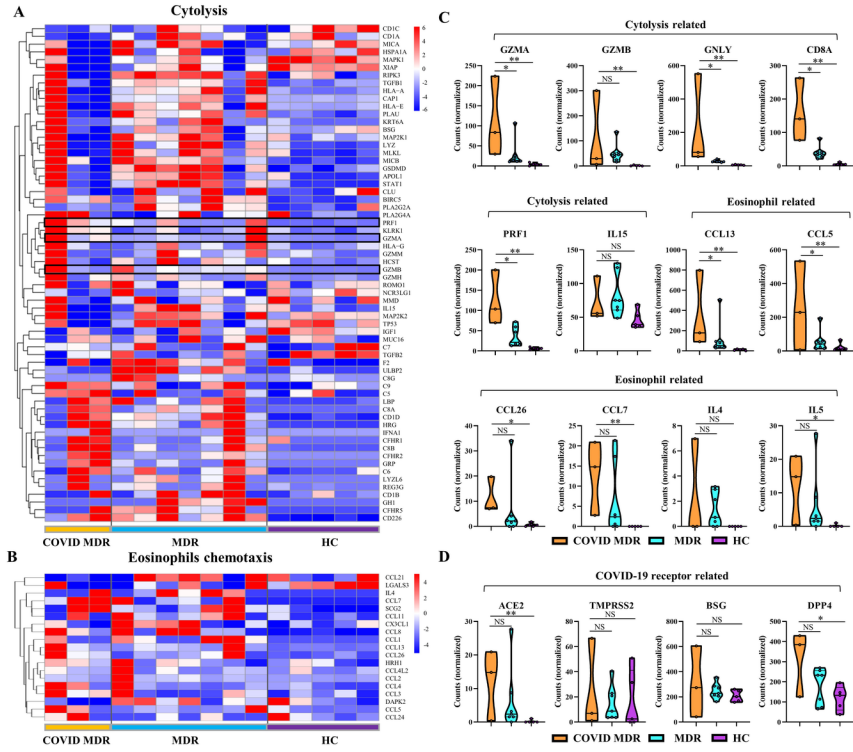
Figure S5. Protein-protein interaction network are depicting upregulated differentially expressed proteins ($p \leq 0.05$, $|\text{L2FC}| \geq 1$) in COVID-MDR, DRESS, and MDR versus HC using STRING online database.



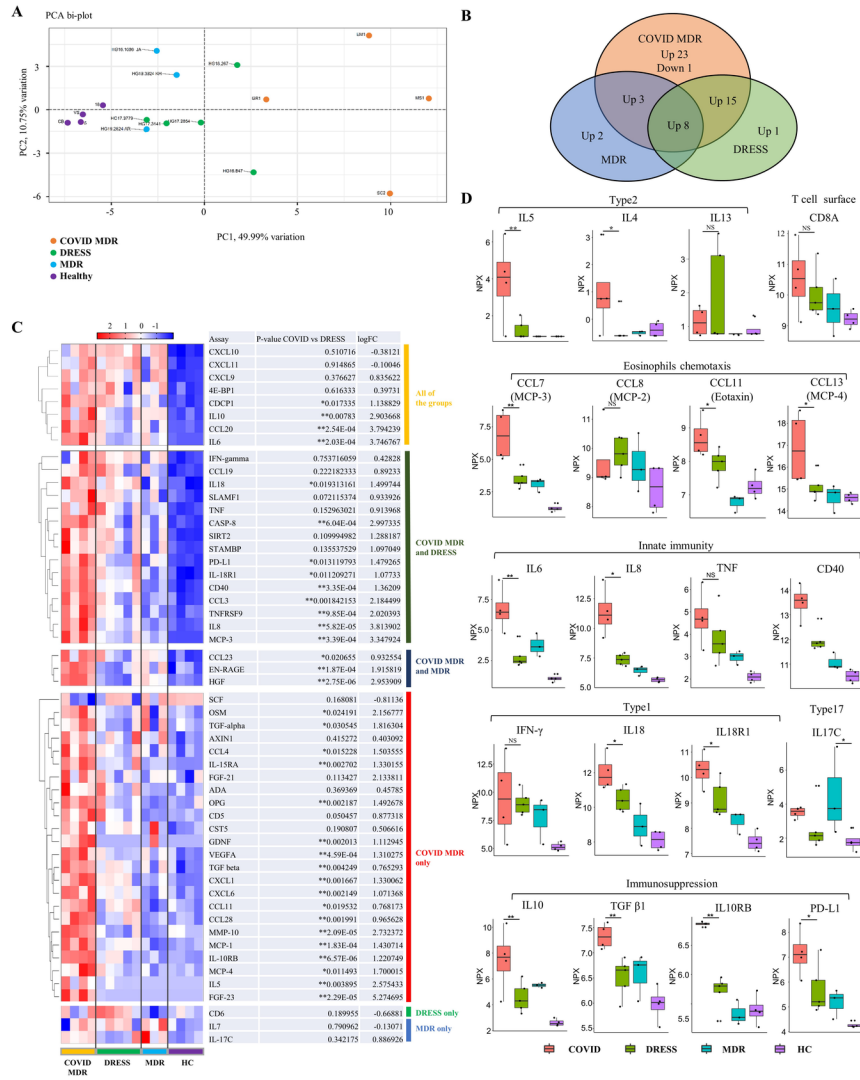
Mitamura *et al.* Figure 1



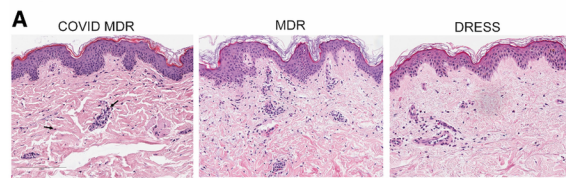




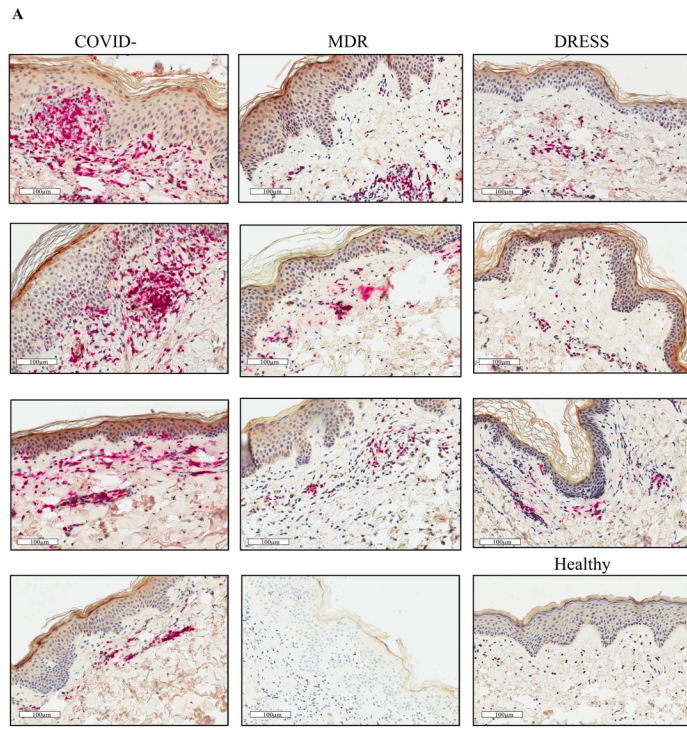
Mitamura *et al.* FIG 4



Mitamura et al. FIG 5



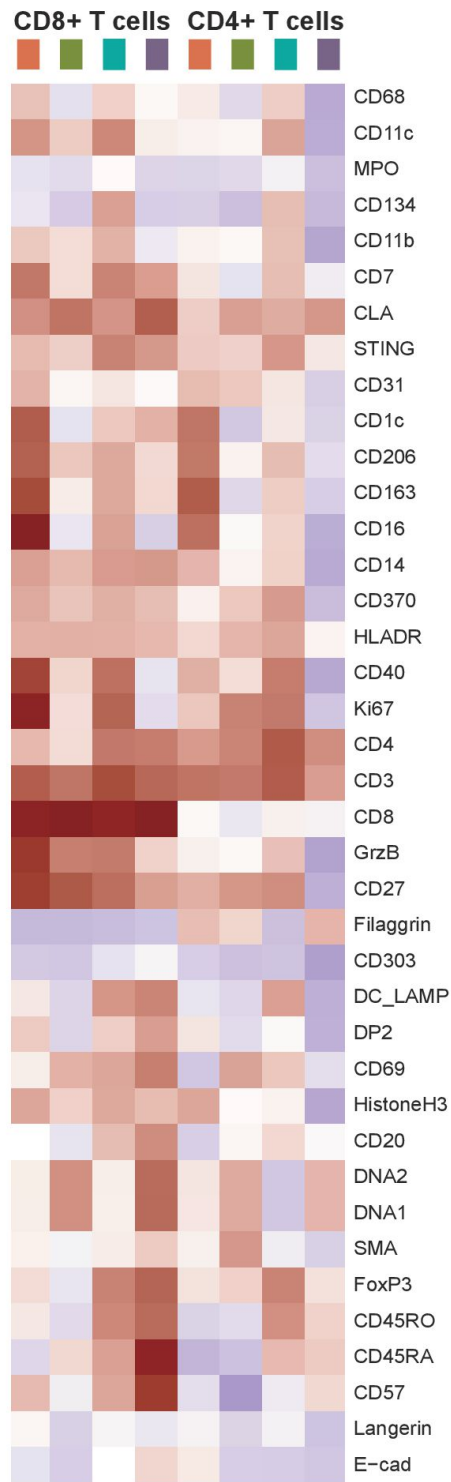
Mitamura et al. Figure S1



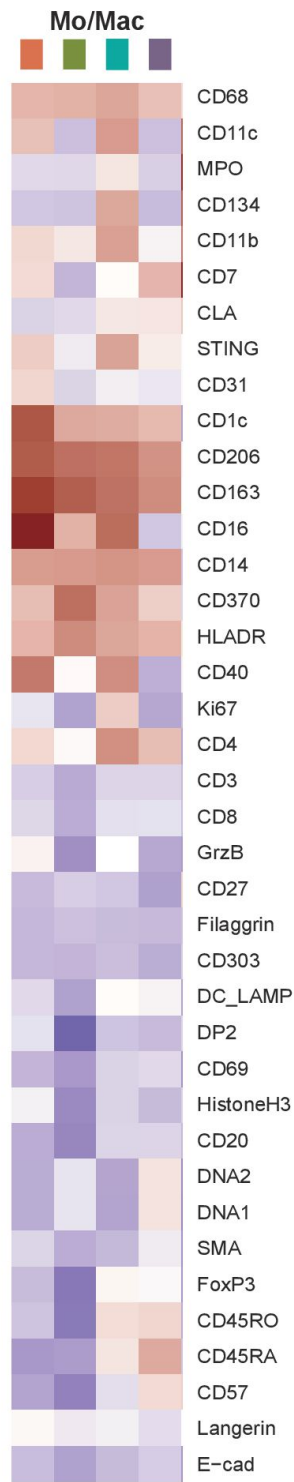
Mitamura et al. Figure S2

FIG S3

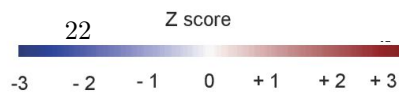
A

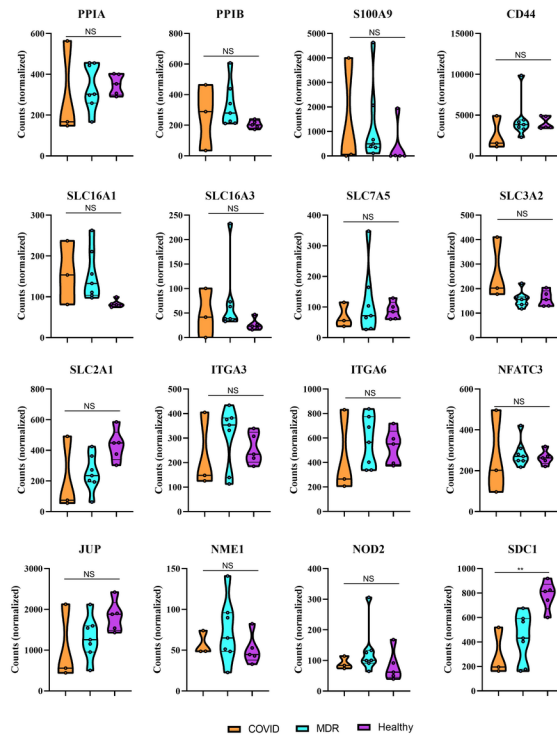


B



■ COVID MDR ■ MDR
■ DRESS ■ HC





Mitamura et al. Figure S4

